PR65, the HEAT-repeat scaffold of phosphatase PP2A, is an elastic connector that links force and catalysis

Alison Grinthal[a], Ivana Adamovic[b], Beth Weiner[a], Martin Karplus[b,c,2], and Nancy Kleckner[a,1]

[a]Departments of Molecular and Cellular Biology, and [b]Chemistry and Chemical Biology, Harvard University, Cambridge, MA 02138; and [c]Laboratoire de Chimie Biophysique, Institut de Science et d'Ingénierie Supramoléculaires, Université de Strasbourg, 67000 Strasbourg, France

Contributed by Nancy E. Kleckner, December 8, 2009 (sent for review October 7, 2009)

PR65 is the two-layered (α-α solenoid) HEAT-repeat (Huntingtin, elongation factor 3, a subunit of protein phosphatase 2A, PI3 kinase target of rapamycin 1) scaffold of protein phosphatase PP2A. Molecular dynamics simulations predict that, at forces expected in living systems, PR65 undergoes (visco-)elastic deformations in response to pulling/pushing on its ends. At lower forces, smooth global flexural and torsional changes occur via even redistribution of stress along the hydrophobic core of the molecule. At intermediate forces, helix–helix separation along one layer ("fracturing") leads to global relaxation plus loss of contact in the other layer to unstack the affected units. Fracture sites are determined by unusual sequences in contiguous interhelix turns. Normal mode analysis of the heterotrimeric PP2A enzyme reveals that its ambient conformational fluctuations are dominated by elastic deformations of PR65, which introduce a mechanical linkage between the separately bound regulatory and catalytic subunits. PR65-dominated fluctuations of PP2A have the effect of opening and closing the enzyme's substrate binding/catalysis interface, as well as altering the positions of certain catalytic residues. These results suggest that substrate binding/catalysis are sensitive to mechanical force. Force could be imposed from the outside (e.g., in PP2A's response to spindle tension) or arise spontaneously (e.g., in PP2A's interaction with unstructured proteins such as Tau, a microtubule-associated Alzheimer's-implicated protein). The presented example supports the view that conformation and function of protein complexes can be modulated by mechanical energy inputs, as well as by chemical energy inputs from ligand binding. Given that helical-repeat proteins are involved in many cellular processes, the findings also encourage the view that mechanical forces may be of widespread importance.

helical-repeat protein | protein elasticity | protein mechanotransduction | spindle tension

Mechanical forces are known to play critical roles in a variety of processes, e.g., cytoskeletal dynamics, opening/closing of membrane channels, effects of torsional superhelical stress in DNA, and effects of spindle tension on chromosome segregation (1–3, reviewed in 4; 5–9). Mechanical inputs are likely to be important in a wider range of cellular processes, involving forces generated by dynamic processes throughout the cell [e.g., for chromosomes (10–12)] or spontaneous thermal fluctuations. In this view, there should be many (more) molecules, some already characterized with respect to biochemical activities, that sense and transduce mechanical stress. Here, using *in silico* molecular dynamics analysis, we have investigated the possibility that HEAT-repeat [Huntingtin, elongation factor 3, a subunit of protein phosphatase 2A, PI3 kinase TOR (target of rapamycin 1)] proteins might be such molecules.

A HEAT repeat is a short pair of interacting helices linked by a tight 1–3 residue (*intra*unit) turn (Fig. 1*A*). HEAT repeats occur in linear arrays, sometimes of 50 or more units. Adjacent units are linked by short (*inter*unit) turns and stacked into two-layered arrays that tend to assume a solenoidal shape (e.g., as in the curved shape of PR65, Fig. 1*B*). This shape is maintained by a network of van der Waals interactions that comprises the hydrophobic "core" of the protein and the interhelix turns. Proteins of other helical-repeat families, e.g., armadillo, translocated promoter region, and ankyrin form analogous structures (13, 14).

Potential for elastic behavior of HEAT-repeat molecules is suggested by (*i*) their solenoidal shapes evocative of a Slinky-like "spring" (14–19), and (*ii*) their involvement in reactions involving DNA and membranes, both readily deformable and thus susceptible to an elastic protein/substrate response, e.g., Ataxia telangiectasia and Rad3 related and TOR (15), and cohesin and condensin (e.g., 20–22). Further, TOR responds to plasma membrane deformations (e.g., 23); and the HEAT-repeat protein PR65 is the scaffolding subunit for PP2A, which is directly implicated in responses to spindle tension [e.g., (8); see below]. Also, ankyrins have recently been shown to exhibit elastic shape changes, raising the question as to their potential mechanical roles (24, 25).

Helical-repeat proteins, including HEAT-repeat proteins, occur in all cellular compartments and are involved in a wide variety of reactions relating to all aspects of cellular function (13, 14, 26). They occur in multicomponent complexes, often serving as scaffolds that bring proteins in contact with other proteins or other biomolecules, e.g., nucleic acids (14, 27). Further, a HEAT-repeat-scaffolded complex, and sometimes the HEAT-repeat molecule itself, has a catalytic function (13, 15). Thus, the demonstration of mechanical modulation of such a molecule, in a particular context (e.g., below), would, by extension, encourage the view that mechanical forces are of biological importance.

This study uses molecular dynamics and normal mode analysis (28–31) to probe the mechanical properties of a prototype HEAT-repeat protein, PR65, alone and as part of its cognate scaffolded complex, the heterotrimeric protein phosphatase PP2A, which is involved in a wide range of cellular processes (32, 33). Differences in PR65 conformation among existing crystal structures are well described by superposition of normal modes. Given that PP2A is an enzyme, an examination of this case also permits investigation of potential relationships between mechanical force and catalysis.

Prior studies of molecular mechanosensory properties focused almost exclusively on tension-induced extension (e.g., 4, 34, 35). The present simulations consider compression, as well as extension, and torsional as well as flexural changes. We also note that some of these studies show that such simulations accurately predict the overall experimental responses of several molecules, including another helical-repeat molecule, and permit unique insights into their properties (e.g., 25, 31, 36).

Author contributions: A.G., I.A., M.K., and N.K. designed research; A.G., I.A., M.K., and N.K. performed research; A.G., M.K., and N.K. contributed new reagents/analytic tools; A.G., I.A., M.K., and N.K. analyzed data; and A.G., B.W., M.K., and N.K. wrote the paper.

The authors declare no conflict of interest.

[1]To whom correspondence may be addressed at: Department of Molecular and Cellular Biology, Harvard University, Fairchild 301, 7 Divinity Avenue, Cambridge, MA 02138; E-mail: kleckner@fas.harvard.edu.

[2]To whom correspondence may be addressed at: Department of Chemistry and Chemical Biology, Harvard University, Conant Chemistry Lab, 12 Oxford Street, Cambridge, MA 02138; E-mail: marci@tammy.harvard.edu.

This article contains supporting information online at www.pnas.org/cgi/content/full/0914073107/DCSupplemental.

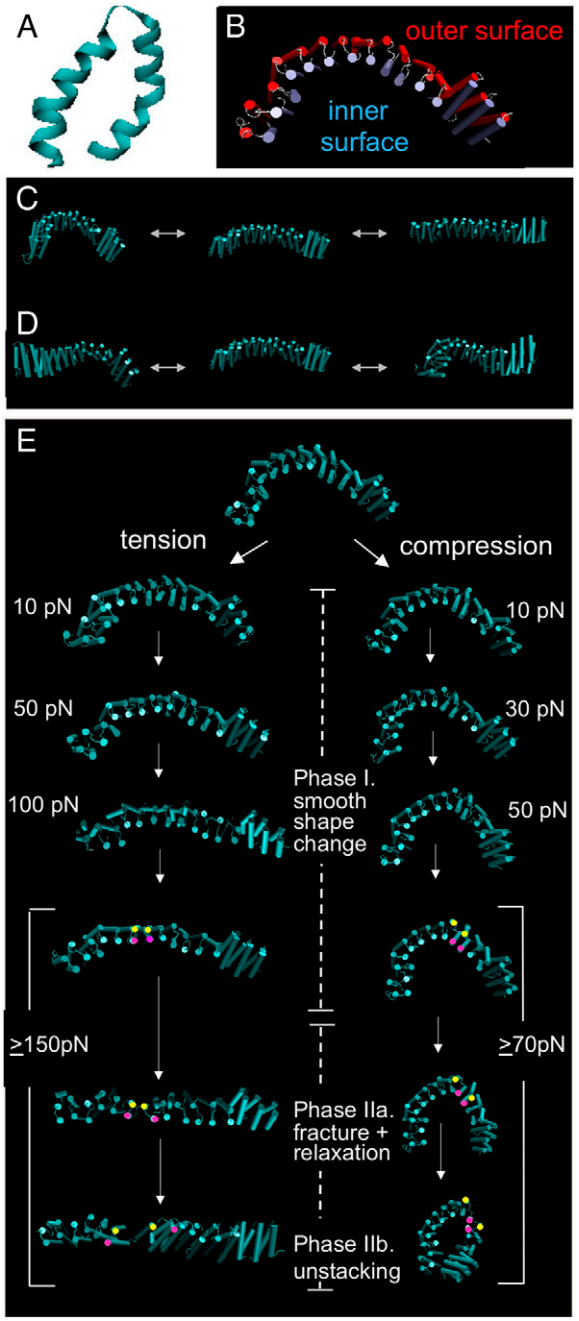

Fig. 1. Effects of tension and compression imposed on the ends of HEAT-repeat protein PR65. (*A*) Single HEAT repeat comprises two interacting α-helices connected by a short interhelix turn. (*B*) Inner (blue) and outer (red) surfaces of PR65: Parallel stacking of repeat units gives rise to a solenoid-like structure with an inner and an outer layer of helices, a ridge of intrarepeat turns along the "top," and a ridge of interrepeat turns along the "bottom." (*C*) First normal mode of PR65 in isolation: global bending/straightening. (*D*) Second normal mode of PR65 in isolation: bidirectional global twisting. (*E*). Top: equilibrated PR65 structure. Bottom: Effects of pulling (left) or pushing (right) on N- and C-terminal Cα atoms along the main axis of the protein with the indicated forces (details in the text).

Results

Pulling or Pushing on the Ends of PR65 Triggers Interconnected Global and Local Changes. Molecular dynamics simulations were used to explore the response of PR65 to externally imposed force. Simulations applied constant pulling or pushing forces to the ends of the protein along its main axis over timescales of nanoseconds at a temperature of 300 K (details in *SI Methods*). All of the reported effects are readily discernible by visual inspection of relevant simulations and are quantified below.

Phase I: smooth straightening/bending. At low pulling or pushing forces, PR65 undergoes progressive smooth straightening or bending (Fig. 1*E*, phase I). These effects are manifested in a progressive change in the end-to-end length of the protein for the first ∼50 ps followed by a plateau at a length directly related to the magnitude of imposed force (Fig. S1). The involved changes alter neither the secondary structure of the molecule nor the overall helix packing that provide the continuous hydrophobic core and overall topology of the protein.

The occurrence of smooth shape changes, rather than discrete local hinge-like motion, although visually apparent, can be quantified in two ways. First, pulling-induced straightening is accompanied by an increase in the interrepeat helix–helix distance at every position along the inner surface and a decrease in the interrepeat helix–helix distance at every position along the outer surface of the protein (Fig. 2*A*). Pushing-induced bending has the opposite effects (Fig. 2*B*). These effects fit with prior studies indicating that the shapes of α–α solenoid molecules reflect variations in interunit distances (37). Second, the local angles formed by each set of three adjacent repeats exhibit small (4–9°), evenly distributed changes.

Shape changes occur without any change in the overall contour length of the molecule. The two helix layers exhibit compensatory, mirror-image length changes whose average is constant as is the end-to-end length calculated from the line through the centers of mass of the repeats (e.g., Fig. 2*C*). Furthermore, global effects do not involve major changes within individual repeat units, either along individual α-helices or in relationships between helices within a unit, which are minimal (Fig. S2). Instead, changes in curvature result primarily from coordinated reorientations between adjacent helices plus small adjustments of their internal structures. The smoothness of the observed shape changes is particularly striking given the structural inhomogeneity of the molecule, with discontinuities involving nonparallel packing of adjacent HEAT-repeat units 3–4 and 12–13 (38).

Thus, mechanical stress imposed at the ends of the protein is uniformly redistributed along its length via the continuous hydrophobic core of van der Waals contacts between helices in the same layer and between the two helix layers.

Phase II: local abrogation of a helix–helix interface followed by relaxation and interunit unstacking. Above a critical force threshold (∼150 pN for pulling; ∼70 pN for pushing), PR65 first undergoes maximal phase I straightening/bending followed by three additional changes that occur in rapid succession (Fig. 1*E* and Fig. S1). First, contact is lost between two adjacent helices, along

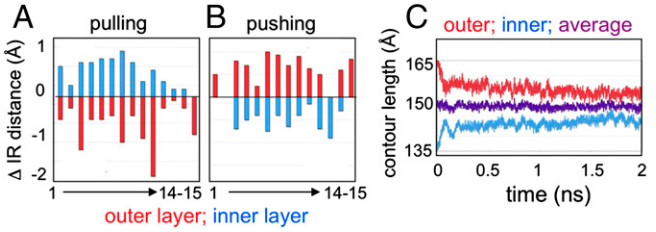

Fig. 2. Straightening and bending result from compensatory tensile and compressive strains in opposite helix surfaces along the entire length of the protein. (*A–B*) Changes in interrepeat distances after pulling at 100 pN (*A*) or pushing at 50 pN (*B*), each measured as the change in distance between adjacent helices, in the inner (blue) or outer (red) layers. Abscissa indicates each pair of repeats for which a change is reported in a corresponding bar. (*C*) Contour lengths for inner (blue) and outer (red) layers, and average of the two (purple), vs time at 100 pN. Contour lengths are the sum of the individual interrepeat distances described in (*A–B*) above.

one helix layer, a change we thus refer to as fracturing. This effect occurs between the "inner layer" helices of units 6–7 for pulling and the "outer layer" helices of units 9–10 for pushing (Fig. 1*B* and *E*). Second, this helix–helix separation is followed nearly instantaneously (Fig. 3) by relaxation along the adjacent regions of both helix layers. Third, in the case of pulling, concomitant with relaxation, contact is lost along the second helix layer opposite the original site, thus unstacking the two involved adjacent HEAT-repeat units.

This progression of changes is reflected quantitatively in the distances between repeats 6–7 and between the ends of flanking segments, as shown for pulling in Fig. 3*A* and *B*. The inner layer 6–7 distance increases during the first 50 ps (phase I straightening), increases further due to the first phase II helix–helix separation (small "x"), and continues to increase as the separation widens until, at ~100–125 ps, unstacking occurs (large "X"). End-to-end distances for the two flanking regions, units 3–6 and 7–12, also increase during phase I but then decrease, concomitant with the first helix–helix separation (arrows), in accord with restoration of curvature. Analogous behavior is observed at 150 and 200 pN, and for pushing at 70 and 100 pN.

These findings imply that stress imposed on the ends of the molecule is redistributed along its length and, at sufficiently high force, promotes local fracturing at a particularly stress-sensitive point ("flaw"). Fracturing occurs along one helix layer but alleviates stress along the entire hydrophobic core of the protein. The resulting relaxation restores curvature, showing directly that mechanical stress is communicated both along and between the two helix layers. Additionally, the local mechanical load at the fracture site is increased due to loss of stabilizing helix–helix contacts such that continuity is soon also lost at the opposing helix–helix interface. With additional time in the presence of the same pulling/pushing force, no additional fractures occur, as expected from global relaxation of the molecule (further discussion below).

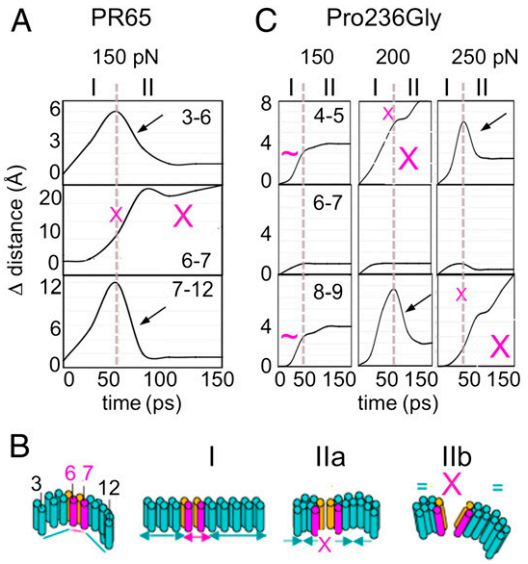

Fig. 3. Fracturing, relaxation, and unstacking in wild-type PR65 and the Pro236Gly mutant. (*A* and *B*) Wild-type PR65; (*C*) Pro236Gly. In (*A*) and (*C*), distances between the indicated HEAT-repeat units (6–7, 4–5, or 8–9) or between the terminal units of segments 3–6 and 7–12 are shown as a function of time after onset of pulling at the indicated forces. Vertical dashed line and small "x" indicate time of fracturing. Large "X" indicates time of unstacking. Arrows indicate relaxation back to curved structure. In (*C*), "~" indicates partial loss of contact between helices in the inner helix layer at 150 pN at 4–5 and 8–9. (*B*) Entire progression of changes for wild-type PR65 (see also Fig. 1*E*, left side). Left to right: original curved structure, global straightening, inner surface fracture at 6–7 accompanied by relaxation of 3–6 and 7–12 segments, and unstacking at the 6–7 interface without further change in adjacent segments.

Interestingly, also, relaxation following fracturing does not fully restore the zero force structure, reflecting the viscoelasticity of the system (Fig. S3; see below).

None of the above changes involve loss of secondary structure. At significantly higher pulling forces (300 pN), terminal helices do unfold. Terminal unraveling during pulling has been observed for other proteins at lower forces, e.g., for spectrin (39, 40) and talin (41). In PR65, this change likely occurs only after phase I/II events because the double layer of helices provides enhanced mechanical stability.

Sites of Fracturing are Determined by Irregular Interhelix Turns. The two residue turn between units 6 and 7, where fracturing occurs, contains a proline, whereas most other interunit turns contain a glycine (Fig. S4*A* and *B*; see also ref. 42). Pushing separates units 9 and 10; the intraunit turn of unit 9 also contains an atypical amino acid (Fig. S4*A* and *B*). To test whether there is a cause-and-effect relationship between irregular turns and fracturing, proline 236 in the 6–7 turn was computationally mutated to a glycine and the simulations under force were repeated.

In the mutant Pro236Gly molecule, helix–helix separation no longer occurs at the 6–7 site: the 6–7 distance increases during phase I, as in the nonmutant protein, but phase II changes are absent (compare Fig. 3*A* with Fig. 3*C*, all forces, middle row). Instead, helix–helix separation occurs again along one helix layer but now at either of two new positions, between units 4–5 or 8–9, and only at higher forces. With pulling at 150 pN, both sites undergo the phase I distance increase and then exhibit small further distance increases (Fig. 3*C*, left panel) that reflect partial separation of component helices along the more stretched (inner) helix layer. With pulling at 200 pN, site 4–5 fractures; the 8–9 distance initially increases but then relaxes as 4–5 fractures. With pulling at 250 pN, units 8–9 undergo phase II changes while the 4–5 distance increases and then relaxes (Fig. 3*C*, center and right columns). Thus, fracturing and unstacking can occur at either the 4–5 or 8–9 interfaces, but requires more force than at the wild-type 6–7 interface. In mechanical terms, when the most stress-sensitive flaw is stabilized, less stress-sensitive flaws emerge. The 4–5 and 8–9 interfaces, like the 6–7 interface, exhibit irregular amino acid residues in contiguous interhelix turns (Fig. S4*A*–*C*). Interestingly, partial separation at 4–5 and 8–9 prior to fracturing is accompanied by even greater strain in the intervening region (Fig. S5), further emphasizing the communication of stress along and between the two helix layers.

The patterns described above show that fracturing at one position along the protein precludes fracturing at another position. Thus, the local relief of stress at a fracture site is then redistributed along the molecule, thereby precluding further stress-promoted changes.

Force-Straightened Protein Behaves Like a Viscoelastic Solid The effects of pulling are fully reversible if force is removed immediately after the maximally straightened configuration is achieved (e.g., at 100 pN; Fig. 4*A*). The released protein returns to its original end-to-end length in the same amount of time it took to straighten [Fig. 4*B (i)*], and with a structure indistinguishable from its prepulling state, by the several criteria discussed above. Thereafter, the protein "overshoots" and then oscillates between more and less curved states. Oscillations decrease in magnitude with time and finally converge to a length close to, but slightly larger than, the starting length. Similar effects are seen if the force is released after 0.2 ns of pulling [Fig. 4*B(ii)*]. This result is in accord with the fact that the straightened structure contains stored potential energy that eventually dissipates to other degrees of freedom within the protein, producing a slight deviation from the original structure. A contribution of kinetic energy is ruled out by the fact that randomization of atomic velocities does not change the behavior (Fig. S6).

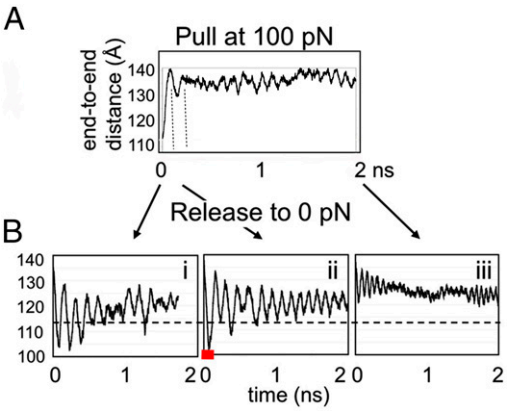

Fig. 4. Force-straightened PR65 behaves as a viscoelastic solid. (*A*) End-to-end distance as a function of time at 100 pN. (*B*) End-to-end distance as a function of time following removal of force. Starting structures for each graph are (from left to right) those obtained after (*i*) 0.05, (*ii*) 0.2, or (*iii*) 2 ns of pulling (above). Horizontal dotted line indicates end-to-end distance before pulling.

In contrast, if the protein is under force for a longer time before release, e.g., 2 ns, the molecule does not return to its original structure on a 2 ns timescale [Fig. 4*B(iii)*]. Thus, with longer time under stress, the molecule is trapped in a new local minimum. The same features are observed for pushing at 50 pN. This behavior implies that PR65 behaves as a viscoelastic solid on the simulation timescale.

PR65 is Intrinsically Prone to Global Flexural and Torsional Changes. Spontaneous protein motions at ambient temperatures can be described approximately by the normal modes of the system (28; *SI Text*, paragraph 1). Such analysis can reveal not only mobilities of individual atoms or within local motifs but also domainal or global (protein-wide) motions in which a larger region, or an entire molecule, exhibits coordinate movement. The most important "modes" defined by such analysis are those of lowest frequency and largest amplitude. In many cases, a small number of modes are sufficient to describe the functionally relevant fluctuations (30). For PR65, the lowest frequency mode (0.37 cm^{-1}) is a uniform, in-plane increase and decrease in the overall curvature (Fig. 1*C*). The second lowest mode (0.81 cm^{-1}) corresponds to an overall twisting motion, which also is distributed uniformly along the length of the structure (Fig. 1*D*). Thus, even in the absence of imposed force, PR65 exhibits intrinsic tendencies for global protein-wide motions. A small number of the lowest frequency modes are able to describe the difference between PR65 by itself and as part of PP2A in the crystal structures as shown using the method of Cecchini et al. (43); see *SI Text*, paragraphs 2 and 3. Thus, the predicted normal modes are relevant to structural changes observed by experiment. Further, the bending and straightening observed under externally applied force is in accord with expectations from the normal mode analysis.

Ambient Conformational Fluctuations of PP2A are Dominated by PR65 Shape Changes that Open and Close the Substrate Binding/Catalysis Interface. We carried out normal mode analysis of a PP2A enzyme comprising PR65, the catalytic (C) subunit and the regulatory subunit B56γ (B′). In the crystallized complex (44, 45), the B and C subunits bind to nonoverlapping regions along the N- and C-terminal halves of PR65, along the edge formed by its intrarepeat turns (Fig. 5*B*, center). The C-subunit catalytic site faces into the thus-created B–C interface, which binds the substrate (Fig. 5*B*, center). The ambient conformational fluctuations of PP2A are dominated by a combination of flexion and torsion of PR65 (Movie S1). In the lowest energy mode of the complex, bending and twisting of PR65, observed in separate modes for PR65 alone (above), are combined into a single motion (Fig. 5*A*; compare with Fig. 1*C* and *D*).

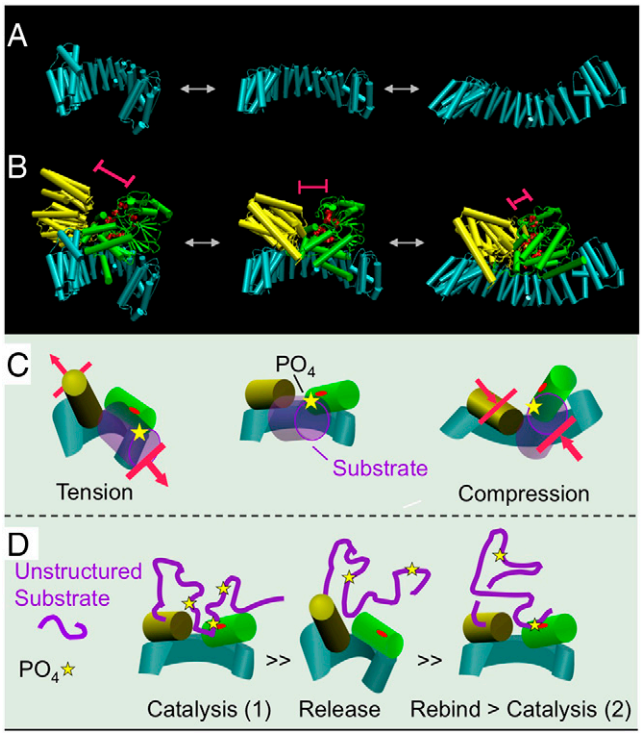

Fig. 5. Ambient conformational fluctuations of PP2A and implications. (*A*) Fluctuations of PR65 as extracted from the lowest normal mode of PP2A (shown in *B*) involve combined flexural and torsional changes corresponding to the lowest modes of PR65 alone (Fig. 1*C* and *D*; see text). (*B*) First normal mode of the PP2A complex (entire motion shown in Movie S1). PR65, cyan; regulatory B56 subunit, yellow; catalytic subunit, green; catalytic active site residues, red. Observed fluctuations are dominated by the changes in PR65 conformation shown in (*A*), which have the effect of opening (left) and closing (right) the substrate/catalysis interface (pink bars). Opening results from motions of the catalytic subunit forward and rightward and the regulatory subunit backward and leftward; closing results from the opposite motions. (*C* and *D*) Proposed mechanisms by which PP2A activity could be regulated by force: externally imposed (*C*) or spontaneous (*D*). In (*C*), the B subunit (yellow) and the substrate (purple) are bound to different subcellular components. When these components are moved in opposite directions by externally imposed force (pink bars plus arrows) the conformation of the substrate/catalysis interface is altered (active site in red; phosphate as yellow star). External tension will promote separation at the interface with concomitant closing of the PR65 elastic connector (left); external compression will promote closer conjunction across the interface with concomitant opening of the PR65 connector (right). For the proposed response of PP2A to spindle tension (see text), movement of B results from association with Shugoshin which moves in opposition to the substrate, cohesin (see text). (*D*). Spontaneous global motions of PR65 could help a B-bound substrate to undergo alternating catalysis ≫ release ≫ rebinding-plus-catalysis, e.g., to promote processive dephosphorylation of multiply phosphorylated proteins such as the unstructured protein (see text).

Importantly, these PR65-dominated motions change the relative dispositions of the B and C subunits, opening and closing the substrate binding/active site interface (Fig. 5*B*). The C subunit is comparatively rigid, but does exhibit internal reorientation of key catalytic residues in concert with the motions of PR65, e.g., Tyr127-Trp200 and Tyr127-His118 distances. These residues have been implicated in PP2A catalysis by mutation studies (46; analogously for related protein PP1, 47). The B subunit, which is also a helical-repeat protein, is more flexible and undergoes limited internal changes in mechanical linkage with PR65.

These results imply that the PR65 scaffold is an elastic connector whose fluctuations are predicted to influence the probability of substrate binding, catalysis, or both. In vivo, such fluctuations could play a role if they were spontaneous or they could be modulated by specific programmed forces generated in the cell (see *Discussion*).

Discussion

The presented results predict that the HEAT-repeat protein PR65 is a (visco-)elastic object, and that its deformations should dominate the intrinsic fluctuations of protein phosphatase PP2A. Further, within PP2A, PR65 is predicted to be an elastic connector that places the regulatory and catalytic subunits in mechanical communication and, more specifically, permits the linkage of force with catalysis.

Mechanical Responses of PR65, a Prototype HEAT-Repeat Protein. In the presented simulations, PR65 behaves as a Hookian spring, undergoing reversible global changes whose magnitude is proportional to the imposed force. These changes reflect the smooth redistribution of stress along the length of the molecule via the core network of van der Waals contacts. In addition, at higher forces, local stress-promoted changes occur at weak points (flaws), with fracturing in one helix layer leading to relaxation along adjacent regions and to loss of contact at the same position in the other layer to produce unstacking. The global effects exemplify "tertiary elasticity" (25, 48), and contrast with "secondary structure elasticity" of other mechanosensitive molecules, e.g., titin, where straightening of linker regions between globular domains is followed by domain unraveling (reviewed in refs. 31, 49–51).

Fracturing involves helix–helix separation. However, the flaws that nucleate fracturing are created by irregularities in interhelix turns. As these turns are very tight (1–3 residues), they introduce conformational restraints on the range of rotational orientations available to the contiguous helices. Consequently, irregularities that create flaws may preclude the formation of optimally stable van der Waals contacts, thereby introducing weak points in the corresponding helix layer. In vivo, if the forces are large enough, the fracturing propensity of a HEAT-repeat protein would be readily tunable by evolution via changes in the sequences of turns. Also, turn length might comprise family specific signatures that modulate the responses of different categories of α–α solenoid/helical-repeat proteins.

Significant changes in PR65 geometry are discernible even with 10 pN of terminally applied force, with fracturing coming into play at ~100 pN. These values are similar to those observed in analogous studies of ankyrin (31). Because molecular dynamics (MD) simulations are limited to nanosecond timescales (e.g., above), higher forces may be required to confer observable effects by this method than would be required over the much longer timescales that are relevant in vivo. For ankyrin, comparison of MD and atomic force microscopy studies suggest that MD simulations overestimate the necessary force level by severalfold (24). Thus, for PR65, forces on the order of piconewtons should have significant effects.

Within PP2A, the PR65 Scaffold is an Elastic Connector That Links Force and Catalysis. Ambient conformational fluctuations of the heterotrimeric PP2A enzyme are predicted to be dominated by elastic conformational fluctuations of PR65. The prominent consequence is (reversible) opening and closing of the B/C interface that mediates substrate binding and catalysis. Orientations of certain catalytic residues in the C subunit are also altered. Thus, PR65 is predicted to be a dynamic, elastic connector, not a rigid structural scaffold. The most interesting implication of the observed effects is that the catalytic activity of PP2A should be reversibly modulatable by force.

Modulation by external force. PP2A activity could be modulated by any effect that moves the B and C subunits in opposite directions, such as motions of two different subcellular elements to which the B subunit and the substrate (and thus the C subunit) are bound (Fig. 5*C*). Such a process could underlie situations in which PP2A activity is responsive to spindle tension. For example, at the second division of meiosis, bipolar pulling forces that arise between the centromere regions of separating chromosomes after anaphase onset are known to cause a centromere-localized molecule (Shugoshin) that binds the B subunit of PP2A to move away from the relevant PP2A substrate, cohesin (8, 52, 53). It thus has been proposed that these oppositely directed movements eliminate PP2A activity by spatially separating the enzyme from its substrate. Our findings suggest a more direct effect in which catalysis is eliminated by deformation of PP2A prior to actual spatial separation (Fig. 5*D*; pink arrows). As required by this model, significant changes in PR65 geometry are expected to occur at force levels that are characteristic of chromosomal processes (11, 54; above) but not so great as to result in dissociation (55). Analogous separations within chromatin (10) (or elsewhere) could modulate other known PP2A activities. Involvement of an elastic connector in modulation of PP2A, with attendant reversibility, would have the advantage of buffering permanent loss of activity against transient imposition of tension (6).

Modulation by spontaneous fluctuations. Alternatively, or in addition, PP2A activity could be modulated by spontaneous fluctuations. If such fluctuations opened the substrate binding/catalytic interface, they could aid in product release, which could be the rate limiting step for PP2A as it is for many enzymes (56). This effect might, for example, contribute to PP2A's activity toward multiply phosphorylated proteins, e.g., the unstructured proteins securin (57) or Tau, whose hyperphosphorylation in the absence of PP2A results in microtubule damage and formation of neurofibrillary tangles diagnostic of Alzheimer's disease (58). Further, under normal conditions, Tau remains bound to the enzyme's B subunit during sequential cycles of capture, catalysis, and release, followed by reconfiguration and capture of another phosphate (58). Fluctuations of PP2A might couple with the motions of Tau to aid in the displacement of one phosphate group by another in the active site. This reaction involves PP2A-B55, which exhibits analogous normal mode fluctuations to PP2A-B56γ (*SI Text*, paragraph 4). Spontaneous opening/closing of the B/C interface could also contribute to exchange of B subunits as required for interconversion among different PP2A holoenzyme species in vivo (e.g., 32).

The mechanical effects observed for PP2A are different from those previously described or proposed in mechanosensory systems (e.g., 4, 5, 35, 41, 50, 51, 59; *SI Text*, paragraph 5) with respect to the specific nature of the relevant motions. Moreover, in PP2A the conformational changes involved are mediated, reversibly, by an elastic connector.

Integration of Mechanical and Chemical Energy Inputs. The current study points to an interesting way of thinking about molecular mechanotransduction. The conformational changes that occur in response to ligand binding are essential elements of protein function (e.g., 60). These changes correspond to an input of energy into the protein. Application of mechanical force and the resultant stress also correspond to an input of energy. Thus, ligand binding and applied force both represent effective energy terms that alter the free energy surface of the protein, stabilizing a different conformation and, thereby, contribute to biochemical function.

We note that some HEAT-repeat proteins are components of complexes that lack catalytic activity. In such cases, HEAT-repeat molecules would be predicted to modulate the overall mechanical properties of their ensembles. For example, cohesin and condensin complexes, both of which include HEAT-repeat-containing subunits, link pairs of chromatin fibers, in chromatin, or in complex arrays along chromosome axes. Involvement of HEAT-repeat domains will give such networks greater elastic coherence than would be conferred by linkages involving rigid tethers connecting highly extensible chromatin/DNA segments (e.g., 61–63).

General Implications for Mechanical Effects in Vivo. The properties described for PR65 are likely to apply to other/all categories of helical-repeat proteins. The principles demonstrated for PR65/PP2A should be broadly applicable to a wide variety of

helical-repeat proteins, helical-repeat-scaffolded complexes, and other types of ensembles in which helical-repeat proteins play important roles. By extension, this raises the intriguing possibility that the cell may contain many tunable elastic molecules whose mechanical properties are crucial for a wide range of functions.

Methods

Computational methods, energy minimization, molecular dynamics simulations, nonequilibrium molecular dynamics simulations, and the methods used to assess changes in relationships between and within repeat units are described in *SI Methods*.

ACKNOWLEDGMENTS. We thank Guido Guidotti for invaluable contributions; Marco Cecchini for performing involvement coefficient and normal mode superposition calculations; Emmanuele Paci for advice on use of the CHARMM program; Felix Koziol for computer assistance; Victor Ovchinnikov for help with movies; Jim Henle for manuscript preparation, Renate Hellmiss for figures, John Hutchinson and Ryan Klock for helpful conversations; and all members of the Kleckner and Karplus laboratories for input. Calculations were performed on the Portal computer cluster at Harvard University. This research was funded by National Institutes of Heath (NIH) Grant R01 GM 025326 (to N.K.), which also supported A.G., and Grant NIH R01-GM030804 (to M.K.); I.A. was supported by NIH Training Grant 5 T32 HL007118-30.

1. Kloda A, et al. (2008) Mechanosensitive channel of large conductance. *Int J Biochem Cell Biol*, 40:164–169.
2. Vollrath M, Kwan K, Corey DP (2007) The micromachinery of mechanotransduction in hair cells. *Annu Rev Neurosci*, 30:339–365.
3. Bianchi L (2007) Mechanotransduction: touch and feel at the molecular level as modeled in Caenorhabditis elegans. *Mol Neurobiol*, 36:254–271.
4. Vogel V, Sheetz MP (2009) Cell fate regulation by coupling mechanical cycles to biochemical signaling pathways. *Curr Opin Cell Biol*, 21:38–46.
5. Li W, et al. (2005) Structure of a synaptic gammadelta resolvase tetramer covalently linked to two cleaved DNAs. *Science*, 309:1210–1215.
6. Nicklas RB (1997) How cells get the right chromosomes. *Science*, 275:632–637.
7. Wan X, et al. (2009) Protein architecture of the human kinetochore microtubule attachment site. *Cell*, 137:672–684.
8. Lee J, et al. (2008) Unified mode of centromeric protection by shugoshin in mammalian oocytes and somatic cells. *Nat Cell Biol*, 10:42–52.
9. Bao G, Suresh S (2003) Cell and molecular mechanics of biological materials. *Nat Mater*, 2:715–725.
10. Kleckner N, et al. (2004) A mechanical basis for chromosome function. *Proc Natl Acad Sci USA*, 101:12592–12597.
11. Lavelle C (2009) Forces and torques in the nucleus: Chromatin under mechanical constraints. *Biochem Cell Biol*, 87:307–322.
12. Wang N, Tytell JD, Ingber DE (2009) Mechanotransduction at a distance: Mechanically coupling the extracellular matrix with the nucleus. *Nat Review*, 10:75–82.
13. Andrade MA, Petosa C, O'Donoghue SI, Muller CW, Bork P (2001) Comparison of ARM and HEAT protein repeats. *J Mol Biol*, 309:1–18.
14. Groves MR, Barford D (1999) Topological characteristics of helical repeat proteins. *Curr Opin Struct Biol*, 9:383–389.
15. Perry J, Kleckner N (2003) The ATRs, ATMs, and TORs are giant HEAT repeat proteins. *Cell*, 112:151–155.
16. Goldenberg SJ, et al. (2004) Structure of the Cand1-Cul1-Roc1 complex reveals regulatory mechanisms for the assembly of the multisubunit cullin-dependent ubiquitin ligases. *Cell*, 119:517–528.
17. Schmidt M, et al. (2005) The HEAT repeat protein Blm10 regulates the yeast proteasome by capping the core particle. *Nat Struct Mol Biol*, 12:294–303.
18. Conti E, Muller CW, Stewart M (2006) Karyopherin flexibility in nucleocytoplasmic transport. *Curr Opin Struct Biol*, 16:237–244.
19. Lee SJ, et al. (2000) The adoption of a twisted structure of importin-beta is essential for the protein-protein interaction required for nuclear transport. *J Mol Biol*, 302:251–264.
20. Neuwald AF, Hirano T (2000) HEAT repeats associated with condensins, cohesins, and other complexes involved in chromosome-related functions. *Genome Res*, 10:1445–1452.
21. Onn I, Aono N, Hirano M, Hirano T (2007) Reconstitution and subunit geometry of human condensin complexes. *EMBO J*, 26:1024–1034.
22. Losada A, Yokochi T, Hirano T (2005) Functional contribution of Pds5 to cohesin-mediated cohesion in human cells and Xenopus egg extracts. *J Cell Sci*, 118:2133–2141.
23. Torres J, Di Como CJ, Herrero E, de la Torres-Ruiz MA (2002) Regulation of the cell integrity pathway by rapamycin-sensitive TOR function in budding yeast. *J Biol Chem*, 277:43495–43504.
24. Lee G, et al. (2006) Nanospring behavior of ankyrin repeats. *Nature*, 440:246–249.
25. Sotomayor M, Corey DP, Schulten K (2005) In search of the hair-cell gating spring: Elastic properties of ankyrin and cadherin repeats. *Structure*, 13:669–682.
26. Maertens GN, Cherepanov P, Engelman A (2006) Transcriptional co-activator p75 binds and tethers the Myc-interacting protein JPO2 to chromatin. *J Cell Sci*, 119:2563–2571.
27. Unsal-Kacmaz K, Makhov AM, Griffith JD, Sancar A (2002) Preferential binding of ATR protein to UV-damaged DNA. *Proc Natl Acad Sci USA*, 99:6673–6678.
28. Brooks BR, Karplus M (1983) Harmonic dynamics of proteins: Normal modes and fluctuations in bovine pancreatic trypsin inhibitor. *Proc Natl Acad Sci USA*, 80:6571–6575.
29. Karplus M, Petsko GA (1990) Molecular dynamics simulations in biology. *Nature*, 347:631–639.
30. Cui Q, Bahar IE (2006) *Normal Mode Analysis: Theory and Applications to Biological and Chemical Systems* (Chapman & Hall/CRC Press, Boca Raton, FL).
31. Sotomayor M, Schulten K (2007) Single-molecule experiments in vitro and in silico. *Science*, 316:1144–1148.
32. Janssens V, Longin S, Goris J (2008) PP2A holoenzyme assembly: In cauda venenum (the sting is in the tail). *Trends Biochem Sci*, 33:113–121.
33. Virshup DM, Shenolikar S (2009) From promiscuity to precision: Protein phosphatases get a makeover. *Mol Cell*, 33:537–545.
34. Johnson CP, Tang HY, Carag C, Speicher DW, Discher DE (2007) Forced unfolding of proteins within cells. *Science*, 317:663–666.
35. Zhang Z, Halvorson K, Zhang C-Z, Wong WP, Springer TA (2009) Mechanoenzymatic cleavage of the ultralarge vascular protein von Willebrand Factor. *Science*, 324:1330–1334.
36. Li L, Wetzel S, Plückthun A, Fernandez JM (2006) Stepwise unfolding of ankyrin repeats in a single protein revealed by atomic force microscopy. *Biophys J*, 90:L30–32.
37. Kajava AV (2002) What curves a-solenoids? Evidence for an α-helical toroid structure of Rpn1 and Rpn2 proteins of the 26 S proteasome. *J Biol Chem*, 277:49791–49798.
38. Groves MR, Hanlon N, Turowski P, Hemmings BA, Barford D (1999) The structure of the protein phosphatase 2A PR65/A subunit reveals the conformation of its 15 tandemly repeated HEAT motifs. *Cell*, 96:99–110.
39. Paci E, Karplus M (2000) Unfolding proteins by external forces and temperature: The importance of topology and energetics. *Proc Natl Acad Sci USA*, 97:6521–6526.
40. Ortiz V, Nielsen SO, Klein ML, Discher DE (2005) Unfolding a linker between helical repeats. *J Mol Biol*, 349:638–647.
41. del Rio A, et al. (2009) Stretching single talin rod molecules activates vinculin binding. *Science*, 323:638–641.
42. Mattos C, Petsko GA, Karplus M (1994) Analysis of Two-Residue Turns in Proteins. *J Mol Biol*, 238:733–747.
43. Cecchini M, Houdusse A, Karplus M (2008) Allosteric communication in myosin V: From small conformational changes to large directed movements. *PLoS Comput Biol*, 15:e1000129.
44. Xu Y, et al. (2006) Structure of the protein phosphatase 2A holoenzyme. *Cell*, 127:1239–1251.
45. Cho US, Xu W (2007) Crystal structure of a protein phosphatase 2A heterotrimeric holoenzyme. *Nature*, 445:53–57.
46. Myles T, Schmidt K, Evans DR, Cron P, Hemmings BA (2001) Active-site mutations impairing the catalytic function of the catalytic subunit of human protein phosphatase 2A permit baculovirus-mediated overexpression in insect cells. *Biochem J*, 357:225–232.
47. Huang HB, Horiuchi A, Goldberg J, Greengard P, Nairn AC (1996) Site-directed mutagenesis of amino acid residues of protein phosphatase 1 involved in catalysis and inhibitor binding. *Proc Natl Acad Sci USA*, 94:3530–3535.
48. Sotomayor M, Schulten K (2008) The allosteric role of the Ca^{2+} switch in adhesion and elasticity of C-cadherin. *Biophys J*, 94:4621–4633.
49. Gao M, Sotomayor M, Villa E, Lee EH, Schulten K (2006) Molecular mechanisms of cellular mechanics. *Phys Chem Chem Phys*, 8:3692–3706.
50. Vogel V (2006) Mechanotransduction involving multimodular proteins: Converting force into biochemical signals. *Ann Rev Biophys Biomol Struct*, 35:459–488.
51. Puchner EM, et al. (2008) Mechanoenzymatics of titin kinase. *Proc Natl Acad Sci USA*, 105:13385–13390.
52. Gómez R, et al. (2007) Mammalian SGO2 appears at the inner centromere domain and redistributes depending on tension across centromeres during meiosis II and mitosis. *EMBO Rep*, 8:173–180.
53. Gregan J, Spirek M, Rumpf C (2008) Solving the shugoshin puzzle. *Trends Genet*, 24:205–207.
54. Fisher JK, et al. (2009) DNA relaxation as a probe for the intracellular environment. *Proc Natl Acad Sci USA*, 106:9250–9255.
55. Paci E, Caflisch A, Plückthun A, Karplus M Forces and energetics of hapten-antibody dissociation: A biased molecular dynamics simulation study. *J Mol Biol*, 314:589–605.
56. Fersht AR (1998) *Structure and Mechanism in Protein Science: A Guide to Enzyme Catalysis and Protein Folding* (WH Freeman, New York).
57. Sánchez-Puig N, Veprintsev DB, Fersht AR (2005) Human full-length Securin is a natively unfolded protein. *Protein Sci*, 14:1410–1418.
58. Xu Y, Chen Y, Zhang P, Jeffrey PD, Shi Y (2008) Structure of a protein phosphatase 2A holoenzyme: Insights into B55-mediated Tau dephosphorylation. *Mol Cell*, 31:873–885.
59. Gräter F, Shen J, Jiang H, Gautel M, Grubmuller H (2005) Mechanically induced titin kinase activation studied by force-probe molecular dynamics simulations. *Biophys J*, 88:790–804.
60. Karplus M, Kuriyan J (2005) Molecular dynamics and protein function. *Proc Natl Acad Sci USA*, 102:6679–6685.
61. Gerlich D, Hirota T, Koch B, Peters JM, Ellenberg J (2006) Condensin I stabilizes chromosomes mechanically through a dynamic interaction in live cells. *Curr Biol*, 16:333–344.
62. Almagro S, Riveline D, Hirano T, Houchmandzadeh B, Dimitrov S (2004) The mitotic chromosome is an assembly of rigid elastic axes organized by structural maintenance of chromosomes (SMC) proteins and surrounded by a soft chromatin envelope. *J Biol Chem*, 279:5118–5126.
63. Ribeiro SA, et al. (2009) Condensin regulates the stiffness of vertebrate centromeres. *Mol Biol Cell*, 20:2371–2380.